The 2025 World Congress on
Advances in Structural Engineering and Mechanics (ASEM25)
BEXCO, Busan, Korea, August 11-14, 2025

ANALYSES OF SEISMIC DESIGN PARAMETERS FOR PILE SUPPORTED BUILDINGS

*Sumin Song[1)] and Junyoung Ko[2)]

[1)] *Department of Civil Engineering, National Taiwan University, Taipei, Taiwan*
[2)] *Department of Civil Engineering, Chungnam National University, Daejeon, Korea*
[1)] ssm9780@ntu.edu.tw
[2)] jyko@cnu.ac.kr

ABSTRACT

This study analyzed the approximate resonant period coefficients for pile-supported buildings. While existing seismic design codes propose approximate resonant period equations for shallow foundations using pseudo-static analysis, there is a lack of pseudo-static methods considering soil-pile-superstructure interaction (SPSI) for pile-supported structures. Therefore, this research proposed approximate resonant period equations for pile-supported buildings based on experimental and numerical analysis results and compared them with existing design codes.

1. INTRODUCTION

Accurately assessing a building's fundamental period of vibration is a cornerstone of modern seismic designs. This parameter is critical as it directly influences the magnitude of seismic forces a structure will likely experience during an earthquake. A precise estimation of the resonant period is essential for ensuring both the safety of the structure and the economy of its design. Consequently, seismic design codes worldwide, such as ASCE 7, Eurocode 8, and KDS 41 17 00, provide simplified empirical equations to help engineers approximate this period in the preliminary design stage.
However, a significant limitation of these proposed code-based equations is that they have been predominantly developed and calibrated for buildings supported on shallow foundations, implicitly assuming a rigid based condition. A number of structures, specifically high-rise buildings or those on soft soil layers, rely on deep foundations like pile foundations. For these pile-supported structures, the dynamic response is far more complex due to the phenomenon of Soil-Pile-Superstructure Interaction (SPSI). This interaction introduces additional flexibility and damping into the system, which can significantly elongate the structure's effective period compared to an equivalent rigid based condition.

[1)] Post-doctoral
[2)] Associate professor

Neglecting the effects of SPSI can lead to a substantial underestimation of the fundamental period. This inaccuracy can make a result in a non-conservative design, where the actual seismic forces are underestimated, potentially being in a danger the structural integrity during a seismic event. Conversely, overly complex dynamic analyses that fully model SPSI are often time-consuming and computationally expensive for routine design practice. Therefore, a critical gap exists between actual behavior and a pseudo-static method for estimating the resonant period of pile-supported buildings.
This study aims to address this critical gap by developing and proposing new approximate resonant period equations specifically for pile-supported buildings. Leveraging the insights gained from a comprehensive suite of experimental tests and extensive numerical analyses, this research systematically investigates the key parameters influencing the period elongation due to SPSI. The proposed coefficients (C_t and x) based on ASCE 7 equations are formulated to be simple enough for practical application while explicitly accounting for the crucial effects of the soil-pile-superstructure system. This paper will thereby provide a valuable tool for practicing engineers to achieve safer and more efficient seismic designs for pile-supported structures.

2. METHODOLOGIES

This study utilized existing experimental shaking table test results (Song, 2024) and numerical analyses conducted by using FLAC 3D (Ver. 5.01), a three-dimensional finite difference analysis program developed by Itasca in the United States. FLAC 3D can analyze groundwater flow and calculate the response to external forces of a continuum by applying the time domain direct integration method. This analysis program provides built in modulus functions for hysteretic damping and the shear modulus reduction factor (G/Gmax) and damping ratio with the cyclic shear strain (Default, Sigmoidal, and Hardin/Drnevich Models).

2.1 Geometry and Interface Modeling

The numerical analysis in this study modeled geometry and boundary conditions, as illustrated in Figure 1 and 2. The dimensions of the soil were 24m in width, 24m in length, and 11.25m in depth. The piles were modeled in a cylindrical shape with a diameter of 0.4m and a length of 12.5m. The pile points were simulated embedded conditions as following tests condition from -11.25 m to -10.5m in depths. The model represented a soil layer from -10.5m. Furthermore, to minimize the interference effects on boundary condition, the soil was expanded to approximately 24 times of pile diameter in the model. Free-field boundary conditions were applied in order to simulate the infinite boundary in the soil to delete reflection waves.
The building was modeled as a 2-story and 5-story of building to match the experimental model. Buildings have dimensions of 16 m in width, 16 m in length, and 7 m and 15.25 m in height, respectively (Figure 2). The damping ratio for both the piles and the superstructure was set at 5%.

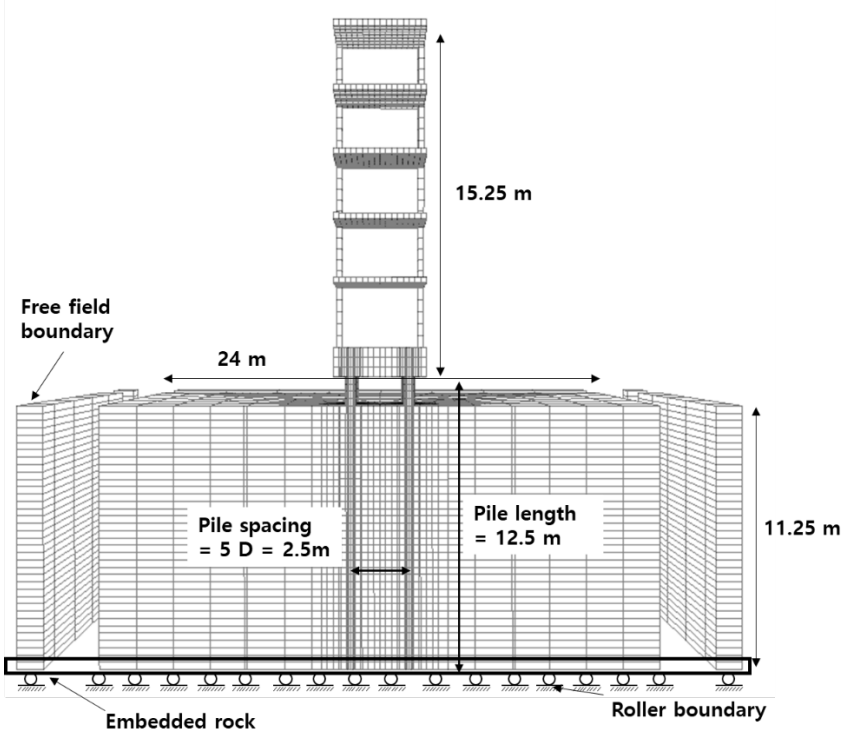

Fig. 1 Cross-sectional view of soil-pile-low story building system

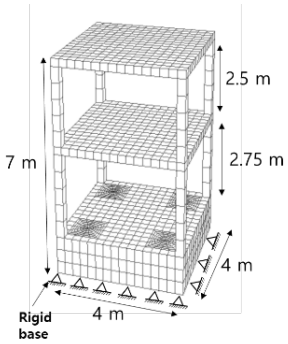

(a) 3rd floor building

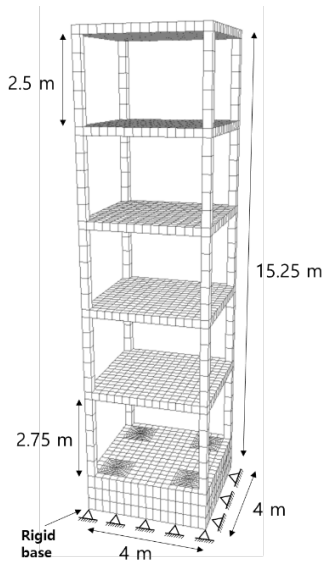

(b) 5th floor building

Fig. 2 Building modeling

In dynamic analysis, the size of the mesh can influence the accuracy of the analysis, especially in terms of the frequency content of the input seismic waves. To account for this, Lysmer and Kuhlemeyer (1969) recommended that the minimum spacing of the mesh be set to be smaller than approximately 1/10 to 1/8 of the highest frequency content of the input wave. Consequently, in this analysis, a maximum mesh spacing of 1.5m was utilized, considering this guideline. Due to the potential occurrence of slippage and separation phenomena at the soil-structure interface under strong external forces during an earthquake, this study used an interface model that could account for interface conditions when seismic events occurred. Figure 3 provides a simplified illustration of the interface model, and the spring coefficients are calculated based on the vertical and shear stiffness of each adjacent element (Itasca, 2009) (Figure 3).

$$k_n = k_s = \left[\frac{K_{near}+\frac{4}{3}G_{near}}{\Delta z_{min}}\right] \quad (1)$$

where, K_{near} and G_{near} is the bulk and shear modulus in adjacent soils, Δz_{min} is the minimum vertical mesh size in contact with interface. K_{near} and G_{near} is the properties considering nonlinear soil behavior by hysteretic model, they can simulate nonlinear soil behavior. In addition, the friction angle of soil-structure interface (δ) was determined by following equation (Beringen et al. 1979),

$$\delta = \phi_{max} - 5° \quad (2)$$

where, ϕ_{max} is the maximum internal friction angle of soil.

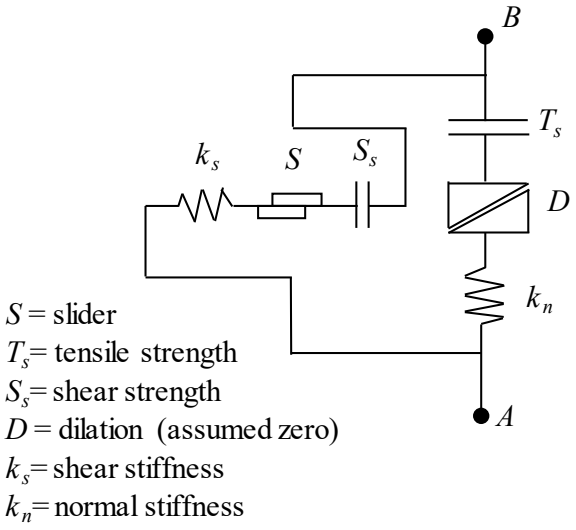

Figure 6.3 Components of the interface constitutive model

2.2 Soil modeling

In this study, the Mohr-Coulomb plasticity model was used as a constitutive model for dry soil condition, and Finn model for an effective stress analysis, was used to evaluate the dynamic behavior of soil-pile-low story building considering liquefaction. Finn model is combined with the Mohr-Coulomb model within FLAC 3D and analysis is performed. When shear strain is applied to undrained saturated soil, it can lead to the generation of excess porewater pressure. This excess pore water pressure occurs to reduce the effective stress within the soil and causes the volume of the soil to expand. The volume change in soil at each cyclic shear strain phase is expressed as following Equation (3) (Martin et al. 1975):

$$\frac{\Delta u \cdot n_e}{K_w} = \Delta\epsilon_{vd} - \frac{\Delta u}{E_r} \tag{3}$$

where, Δu is the increment of pore water pressure, $\Delta\epsilon_{vd}$ is the volumetric increment of soil, E_r is the tangent modulus of unloading curve, n_e is porosity, and K_w is bulk modulus of water (2.2 GPa).

There is various formula to calculate $\Delta\epsilon_{vd}$ in Equation (3), this study used the Equations (4 and 5) proposed by Bryne (1991),

$$\frac{\Delta\epsilon_{vd}}{\gamma} = C_1 \exp\left(-C_2 \frac{\epsilon_{vd}}{\gamma}\right) \tag{4}$$

$$C_1 = 7600(D_r)^{-2.5}, C_2 = 0.4/C_1 \tag{5}$$

where, γ is the shear strain, C_1 and C_2 is the volume change constants, and D_r is the relative density of soil (%). The soil was simulated in this study as Jumunjin sand, C_1 and C_2 used in this study is summarized in Table 1. The particle size distribution curve of Jumunjin sand used in this study is located in the high liquefiable boundary, as suggested by the Japanese Port Structure Seismic Design Standards. (Figure 4). Song et al. (2022) analyzed numerical simulation by FLAC3D according to different soil condition by using properties of Finn model as Table 1.

Table 1 Input properties of soil model used in Finn model

Properties	**Relative density of soil (%)**	
	40	**80**
Porosity	0.42	0.38
Permeability coefficient (m/s)	7.5×10^{-5}	3.7×10^{-5}
Volume change constants	$C_1 = 0.751$ $C_2 = 0.533$	$C_1 = 0.133$ $C_2 = 3.01$

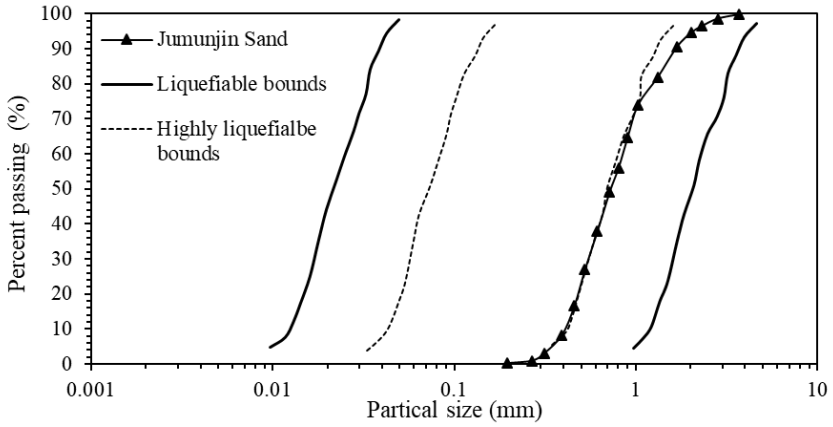

Figure 4 Particle size distribution and liquefaction potential curve

The soil properties are summarized in Table 2. where, ϕ is the internal friction angle of soil (°), ***e*** is the void ratio, γ_d is the dry unit weight of soil (kN/m^3), γ_{sat} is the saturated unit weight (kN/m^3), ν is the poisson's ratio, and V_s is the shear velocity of soil, G_{max} and is the maximum shear modulus of soil (MPa). G_{max} is governed by soil depth, it was calculated by Equation 6. Yoo and Park (2015) proposed the correlation equation along the confining stress between V_s and G_{max} of jumunjin sand by bend element tests (Equation 7), so this study calculated G_{max} by using Equations 6 and 7 (Figure 3).

$$G_{max} = \rho \times V_s^2 \tag{6}$$

$$V_s(m/s) = (300 - 110e) \times \left(\frac{\sigma\prime}{p\prime_a}\right)^{0.25} \tag{7}$$

where, ρ is the density of soil (kg/m^3), ***e*** is the void ratio, p'_a is the atmospheric pressure (≈100 kPa) and σ' is the effective stress.
Kown (2016) obtained G/G_{max} - γ curve of Jumunjin sand from the triaxial test and resonant column test. Based on the test results, they determined the input values L_1 and L_2 necessary for the hysteretic damping model. L_1 and L_2 are the coefficients that determine the decreasing rate and decreasing starting point of the G/G_{max} value in G/G_{max}-γ curve L_1 and L_2 were -3.65 and 0.5, respectively. Figure 4 shows the G/G_{max}-γ curve obtained by applying the default model and damping ratio curve calculated in FLAC 3D.

Table 2 Material properties

Properties	**Sand (D_r =40 %)**	**Sand (D_r =80 %)**	**Rock**	**Pile, Raft and Building**
γ_d (kN/m^3)	14.45	15.82	21	24
γ_{sat} (kN/m^3)	18.73	19.54	21	-
ϕ (◦)	32.7	36.2	-	-
ν	0.3	0.3	-	0.2
e	0.75	0.59	-	-
V_s (m/s)	180	260	-	-
G_{max} (MPa)	18.4-88.1	24.5-117	5,208	26,923
Lateral stiffness, *k* (N/cm)	-	-	-	13,800 /10,368
Mass, *m* (kg)	-	-	-	10,800 (1~ 5th floor)

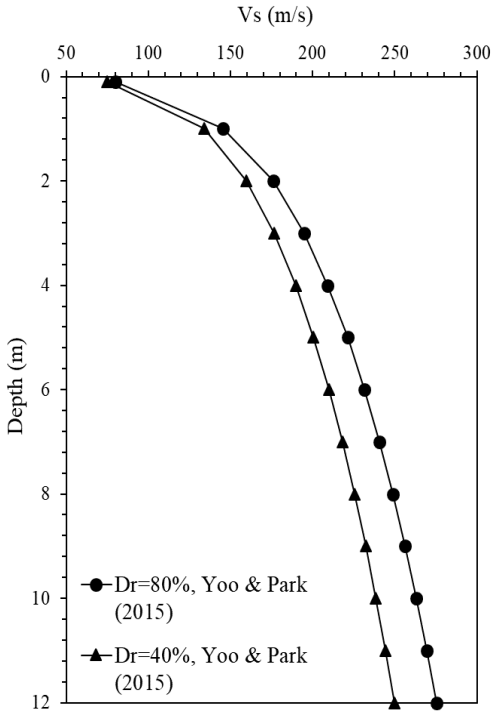

Figure 5 Particle size distribution and liquefaction potential curve

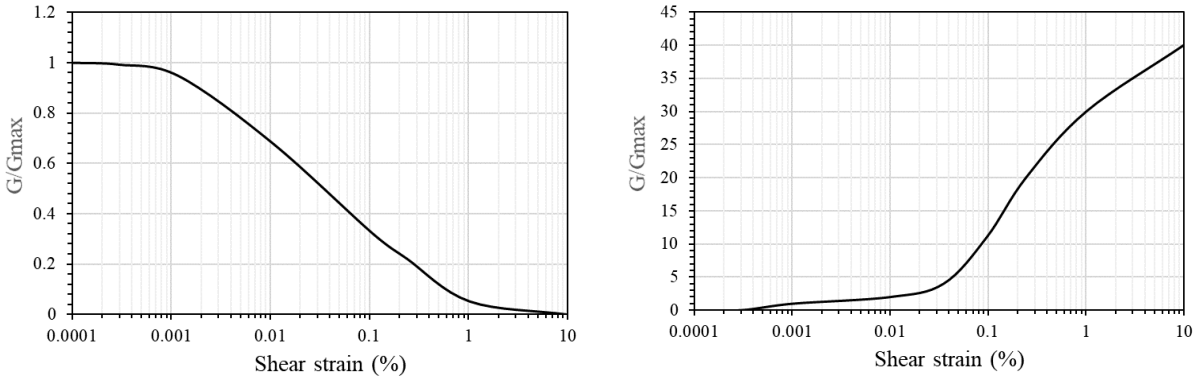

(a) Modulus reduction curve (b) Damping ratio curve

Figure 6 Modulus reduction and damping ratio curve

3. Validation of 3D FDM with Test Results

The validation of the 3D FDM model used in this study was examined by a comparison with the experimental results of the resonant periods in prototype scales (Song, 2024). The soil is modeled Jumunjin sand with the relative density of 80 % as Table 2.

The input acceleration, white noise, was used for accessing the resonant period of building structures. White noise has an equivalent acceleration in all frequency ranges, so the resonant period of building can be calculated by using FFT analyses. White noise in this study has almost 0.05 g amplitude, and its duration time is 3.0 sec (Figure 7).

Figure 8 shows the typical results of response acceleration at the building roofs and its FFT result. The results show that the numerical modeling, small-scale shaking table test results (Song, 2024), and structural design codes have a reasonable correlation (Figure 9). These results show that there is a reasonable agreement between the computed and measured resonant period of the building structure.

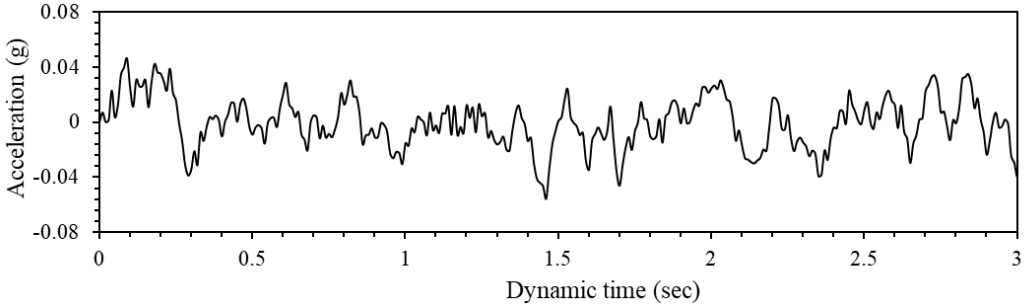

(a) Time historic response acceleration

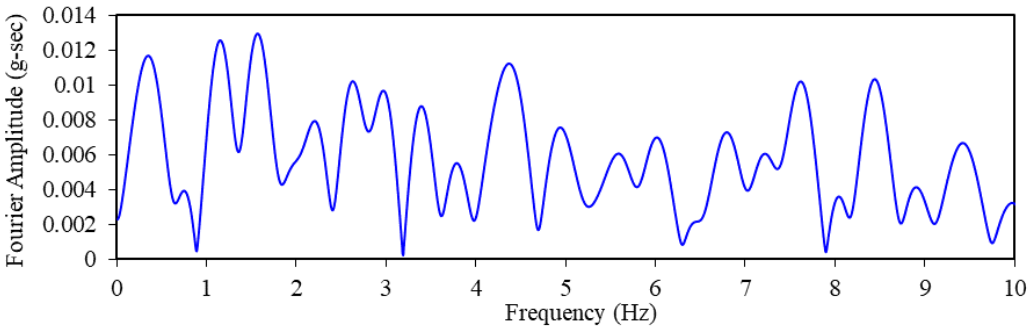

(b) FFT results

Figure 7 Input wave – white noise (input acc. = 0.05 g)

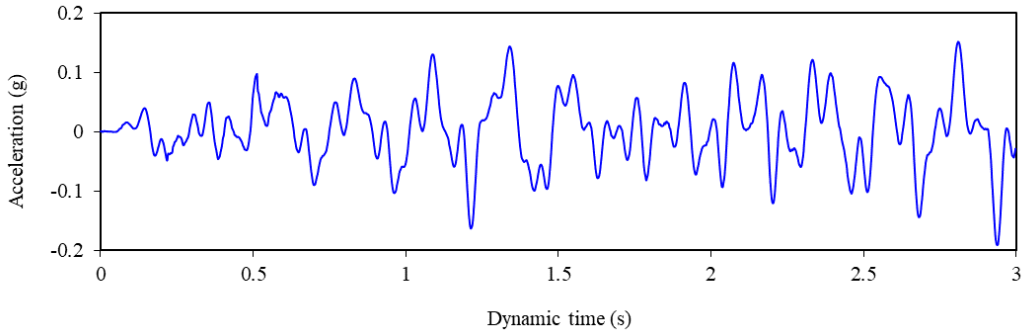

(a) Time historic response acceleration

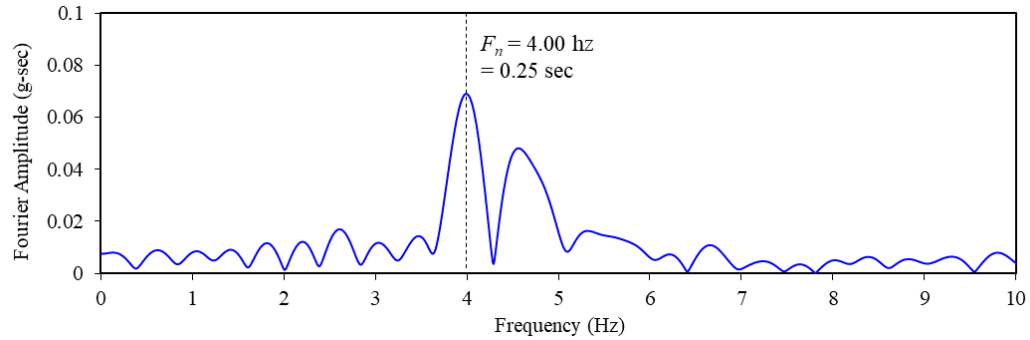

(b) FFT results

Figure 8 Typical white noise analysis results (3-story building – rigid base condition)

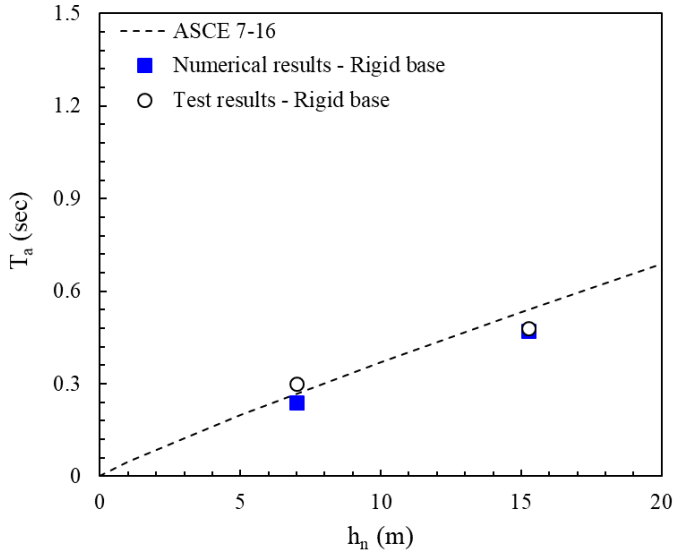

Figure 9 Validation for the resonant period of rigid based models

4. The Resonant period of Soil-Pile-Building Systems

4.1 Analysis Program

Numerical analysis was performed on 2, 5, and 8-story buildings with pile foundation in soil layer to propose approximate period coefficients. The physical properties of the soil layer, piles, and buildings are the same as mentioned above in Table 2. 12 cases of analyses were performed and the detail of analyses programs are summarized as Table 3.

Table 3 Test program of numerical analyses

Cases	Dr (%)	Stories	Groundwater	Input acc. (g)
4	40/80	2	O/X	0.05 White noise – 3 sec
4		5		
4		8		

4.2 Analysis Results

Figure 10 shows the typical analysis results in the pile-supported 5-story building with dense saturated soil. Through white noise tests, the resonant period was calculated as 0.84 sec in this analysis case, and an excess pore water pressure ratio was generated during the dynamic loads. The amount of r_u was almost 0.1 due to the effects of the lower input acceleration, and dense soil condition (Figure 10 (c)).

Figure 11 shows the numerical results of resonant periods of pile-supported building according to soil conditions. Rigid base condition recorded the lowest resonant period than the others in all building heights.

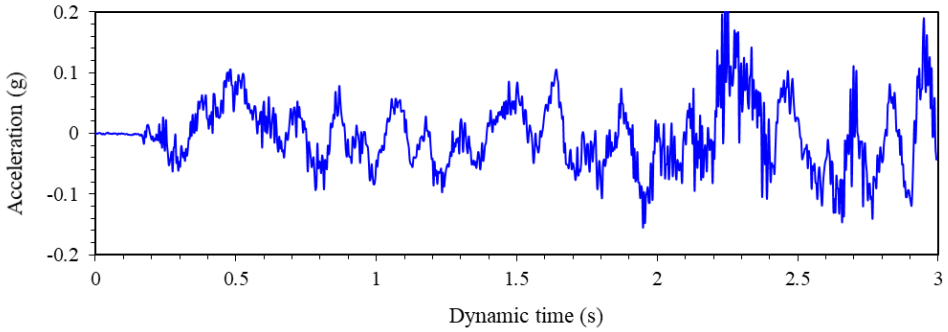

(a) Time historic response acceleration

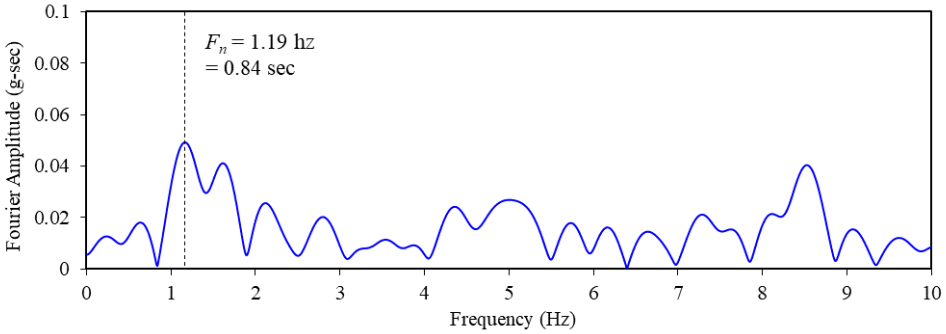

(b) FFT results

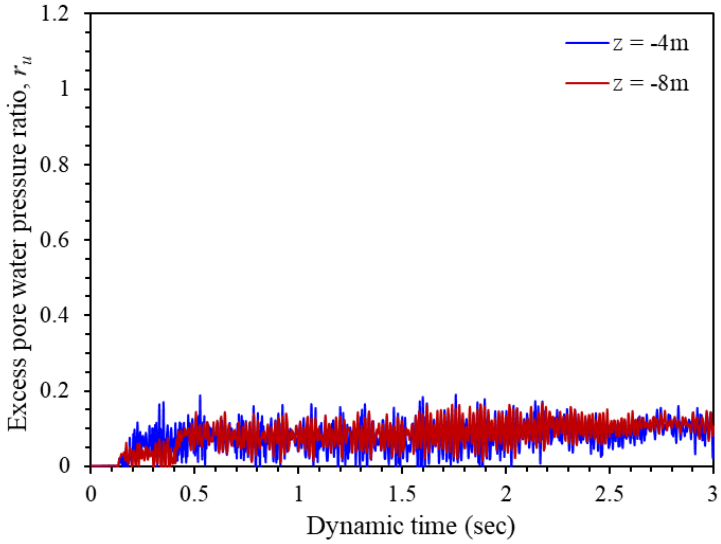

(c) Excess pore water pressure ratio (r_u)

Figure 10 Typical analysis results (6-story building, Dr=80%, Saturated condition)

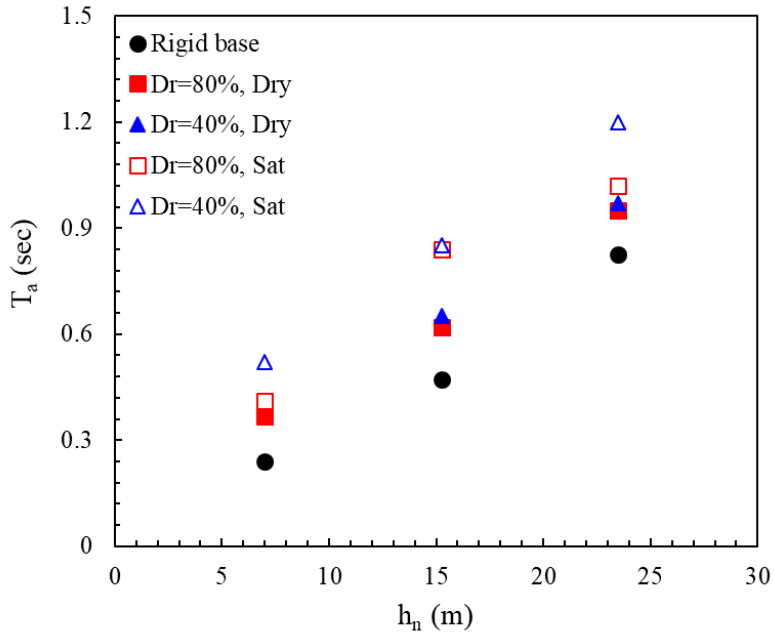

Figure 11 Resonant periods of pile-supported buildings

4.3 Calculated Approximate Period Parameters

As described in previous chapter, the analysis results of the resonant period according to the height of the building are depicted in Figure. Table 6.4 summarized the proposed approximate period parameters (C_t and x). In ASCE 7-16 and KDS 41 17 00, the approximate fundamental period (T_a), in seconds, shall be determined from Equation 8:

$$T_a = C_t {h_n}^x \tag{8}$$

where, h_n is the structural height from the base level, and the C_t and x are approximate period parameters (ASCE 7-16). Following this equation form, this study proposed the approximate period parameters (C_t and x) based on experiments (Song, 2024) and numerical analyses results.

Numerical analysis was performed on a 8-story building to propose approximate period parameters. The physical properties of the soils, piles, and buildings are the same as mentioned above in Table 2. Analysis was performed for rigid base and fixed-pile conditions, and the analysis results of resonant periods is as follows.

The trendline calculated by proposed coefficients is located on the ASCE 7-16, because ASCE 7-16 is for building with rigid base condition.

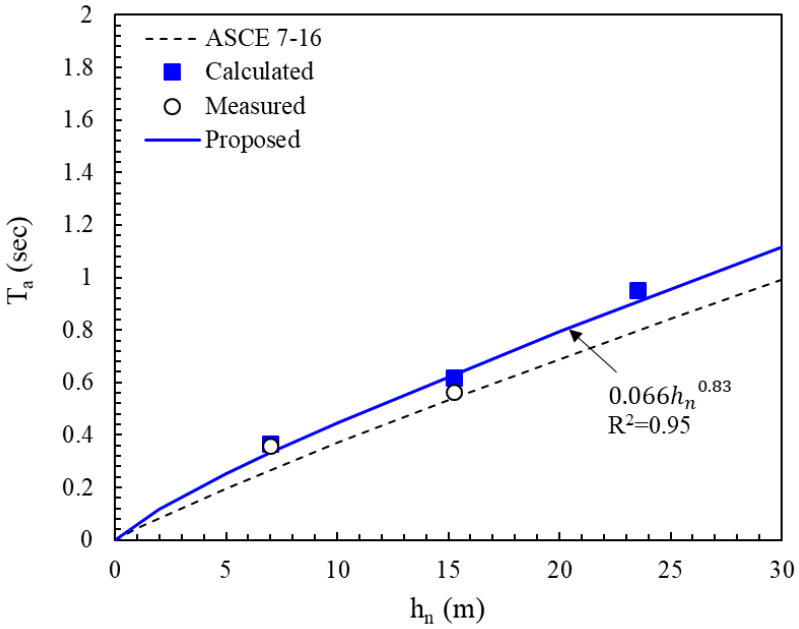

(a) D_r = 80 %, Dry soil

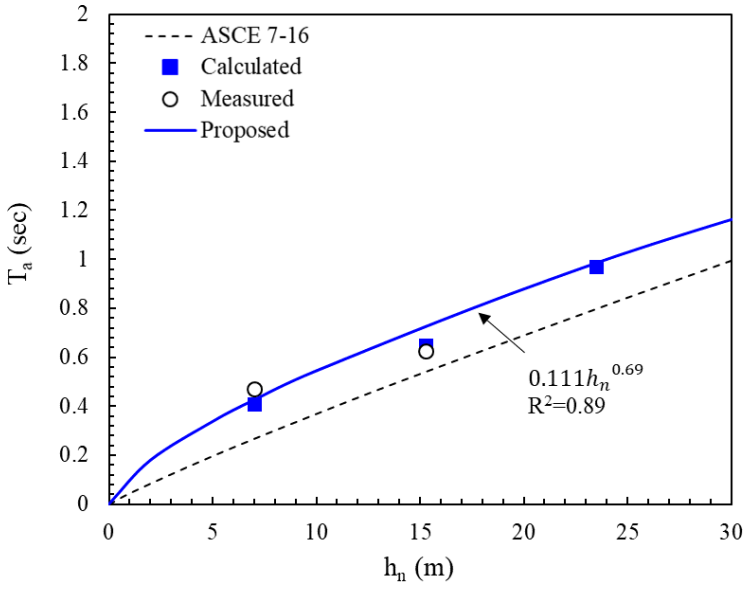

(b) D_r = 40 %, Dry soil

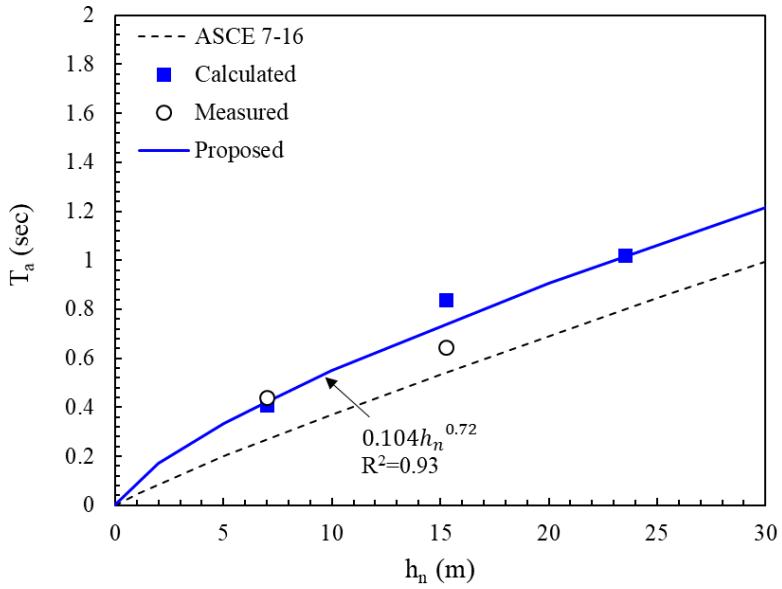

(c) D_r = 80 %, Saturated soil

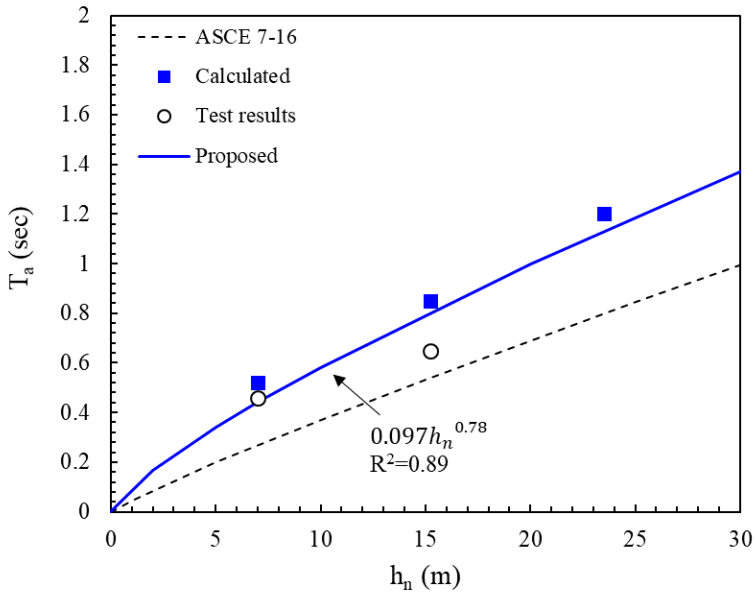

(d) D_r = 40 %, Saturated soil

Figure 6.12 Calculated curves with varying soil conditions

Table 4 Proposed approximate period parameters (C_t and x)

Case	C_t	x
D_r = 80 %, Dry	0.066	0.83
D_r = 40%, Dry	0.111	0.69
D_r = 80%, Saturated	0.104	0.72
D_r = 40%, Saturated	0.097	0.78

5. CONCLUSIONS

The main objective of this study is to analyze the approximate resonant period coefficients numerical analyses. The calculated resonant period of the building with the rigid base was validated with experimental results and seismic design codes. The approximate resonant period coefficients for pile-supported buildings were proposed according to soil conditions. Approximate period coefficients (C_t and x) calculated in this study had a higher resonant period than existing seismic design codes by considering soil-pile-structure interaction.

REFERENCES

ASCE 7-16, (2016), Minimum Design Loads for Buildings and Other Structures.

Beringen, F. L., Windle, D., Van Hooydonk, W. R. (1979), “Results of Loading Tests on Driven Piles in Sand. Recent Developments in the Design and Construction of Piles”, Institute of Civil Engineering (ICE).

Lysmer, J., and Kuhlemeyer, R. L. (1969), “Finite Dynamic Model for Infinite Media”, Journal of the Engineering Mechanics Division, Vol. **95**, No. 4, pp. 859-878.

Martin, G. R., Finn W. D, L., Seed, H. B. (1975), “Fundamentals of Liquefaction under Cyclic Loading”, Journal of Geotechnical and Geoenvironmental Engineering, Vol. **101**, pp. 324-438.

Itasca Consulting Group (2009), FLAC3D (Fast Lagrangian Analysis of Continua in 3Dimensions) User's Guide, Minnesota, USA.

KDS 41 17 00, (2019), Korea Design Standard, Seismic Building Design Code.

Kown, S. Y., Kim, S. J., Yoo, M. T. (2016), “Numerical Simulation of Dynamic Soil-pile Interaction for Dry Condition Observed in Centrifuge Test”, Journal of the Korean Geotechnical Society, Vol. **32**, No. 4, pp.5-14.

Song S., Lim H., Park S., Jeong S., (2022), “Proposed dynamic p-y curves on a single pile considering shear wave velocity of soil”, Earthquake and Structures, Vol. **23**(4), pp.353-361.

Song S., (2024), "Soil-Structure Interaction Analysis of Pile supported Structures by 1g Shaking Table Tests", Ph.D dissertation, Yonsei University, Seoul, Korea.

Yoo J.K., Park D., (2015), “Shear Strength Estimation of Clean Sands via Shear Wave Velocity”, Journal of the Korean Geotechnical Society, Vol. **31**(9), pp. 17-27 (In Korean).